THE VOLTAGE DISCHARGE CHARACTERISTICS OF MANGANESE DIOXIDES

H. W. UHLIG

VEB Berliner Akkumulatoren- und Elementefabrik, Wilhelminenhofstrasse 68/69, 1160 Berlin (G.D.R.)

(Received December 17, 1986; in revised form September 28, 1987)

Summary

On the basis of experimental investigations of electrolytic manganese dioxide (EMD) in the pH range 0 - 15, its voltage as a function of the state of discharge is discussed. A description of the voltage/discharge curves requires four different functions, if Mn(II) formation is considered. For reduction in an homogeneous phase a function based on the classical formula from Johnson and Vosburgh in consideration of the hydration energy is suggested. Comparing the results with other electrode materials a classification of the insertion mechanism is attempted.

Introduction

A determination of the charge density of cathode materials is important for assessing new electrode materials. When applying a factor, q, to reduce the theoretical value, the practical charge density, φ, can be calculated with sufficient accuracy from the specific capacity, c_S, and the crystallographic density, ρ_K, via eqn. (1) [1]

$$\varphi = c_S \rho_K \Pi q_i \quad (1)$$

The factor, q, depending on the electrolyte, the inert material, and the difference between the crystallographic form and the power density can be obtained using empirical values. For applications in which the voltage, U, is limited, the available charge density depends on the voltage characteristic and the factor, q_ϵ, in eqn. (1), as is demonstrated in Fig. 1.

Predicting the charge density of electrode materials therefore presumes the existence of generalised voltage characteristics. Considering the literature, most electrode materials can be classed according to one of three types of electrode reaction using the mode of charge transfer between the solid phase and electrolyte phase:

- type I insertion mechanism (H^+Li^+)
- type II electrolyte phase mechanism (M^{z+})
- type III redox mechanism with activated adsorption (e), and detailed in Table 1.

0378-7753/88/$3.50

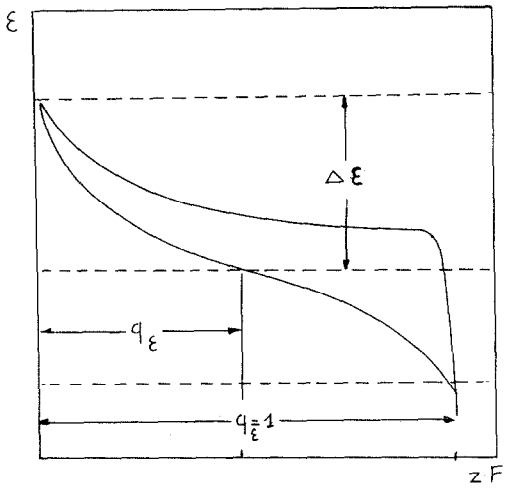

Fig. 1. Voltage as a function of the state of discharge showing the available voltage range $\Delta\epsilon$ expressed by an A h capacity factor q_ϵ.

TABLE 1

Classification of electrode materials

Reaction type	Example	Structure
I	α-MnO_2, ϵ-MnO_2, α-PbO_2	MO_6 octahedra chains with canals
	β-NiOOH, β-FeOOH	layer structure
II	Cu_2O, Ag_2O, ZnO, HgO	cubic, rock salt type
	β-PbO_2, Fe_3O_4	tetragonal, spinel type
	β-MnO_2	rutile type
III	H_2, O_2, Cl_2, I, S	non metals

The voltage of a type I material depends on the degree of oxidation, n:

$$\epsilon(n) = -\frac{1}{F}\left(\frac{\mathrm{d}\Delta G}{\mathrm{d}n}\right) \tag{2}$$

Type II corresponds to a second kind of electrode with a plateau in the voltage characteristic, whereas that of type III can be calculated by the Nernst equation of the cross reaction in the electrolyte phase.

Potential curves within type I electrodes have many forms. In recent years the potential functions of insertion electrodes have been described on the basis of Gibbs equation

$$\Delta G = \Delta H - T\,\Delta S \tag{3}$$

using the change in entropy of inserted protons, lithium ions and electrons. It should, therefore, be possible to interpret potential functions within the

type I group independently of any of the specific properties except for the change in enthalpy, ΔH.

The possibility of such an interpretation will be discussed using MnO_2 as an example in the ϵ- and α-EMD and β-MnO_2 forms which differ in composition and crystal structure. β-MnO_2 is the closest to pure MnO_2, whereas the ϵ- and α-MnO_2 forms contain Mn(III) ions and combined water. In addition, α-MnO_2 contains foreign cations such as K^+ or NH_4^+. The structure consists of MnO_6 chains or double chains, forming canals of different dimensions [2].

In the literature two predominant discharge mechanisms are discussed. Firstly an homogeneous phase reaction of EMD in both weak acid and alkaline solutions presented by Atlung [3] in the form:

$$MnOOH_x + \delta H^+ + \delta e \longrightarrow MnOOH_{x+\delta} \tag{4}$$

and secondly, a mechanism with Mn(II) formation by disproportionation of EMD in acid solutions (pH $\leqslant$ 3) and of β-MnO_2 in a neutral solution [4, 5].

$$2MnO_2 + 2H^+ + 2e \longrightarrow 2MnOOH \tag{5a}$$

$$2MnOOH + 2H^+ \longrightarrow MnO_2 + Mn^{2+} + 2H_2O \tag{5b}$$

$$MnO_2 + 4H^+ + 2e \longrightarrow Mn^{2+} + 2H_2O \tag{5c}$$

The homogeneous phase mechanism, first described by Johnson and Vosburgh [6] on the basis of an homogeneous solution of MnO_2 and MnOOH, is usually written in the form:

$$\epsilon = \epsilon^0 + \frac{RT}{F} \ln \frac{1-x}{x} - 0.059 \text{ pH} \tag{6}$$

with mole fractions x for MnOOH and $1-x$ for MnO_2.

As eqn. (6) does not agree sufficiently well with the experimental results, many attempts have been made to correct the function. Using statistical thermodynamics, the potential slope was recently interpreted as a function of the entropy of independently inserted protons and electrons:

$$\Delta S = k \ln W^2 \tag{7}$$

Using Stirling's approximation to solve this instead of eqn. (6) we get:

$$\epsilon = \epsilon^0 + \frac{2RT}{F} \ln \frac{1-x}{x} - 0.059 \text{ pH} \tag{8}$$

Since eqn. (8) agrees with the experimentally observed potential slope only in the range $x \leqslant 0.5$, it was modified, assuming changes in the configuration of the inserted protons and electrons [3, 7, 8]. Several authors either consider $x = 0.5$ to be the end of the homogeneous phase [9, 10] or assume the existence of a second homogeneous phase [11].

Experimental

The discussion was based on investigations of discharging EMD with ϵ- and α-structure in the pH range 0 - 15, published earlier [12]. Discharge curves and reaction products are presented in Fig. 2 and Table 2. Below a pH of 12 discharge leads to Mn(II) formation, which is delayed in the range $3 < pH < 12$, as shown in Fig. 3. This is in agreement with the results of Kanoh [13].

Mn(II) formation and the voltage discharge characteristic, as shown in Fig. 4, depend on the current density, suggesting that kinetic factors are involved. In the range $3 < pH < 12$ these characteristics consist of an initial section with a falling potential and a second section in which the voltage is nearly constant. Mn(II) solution only proceeds during the second section. In

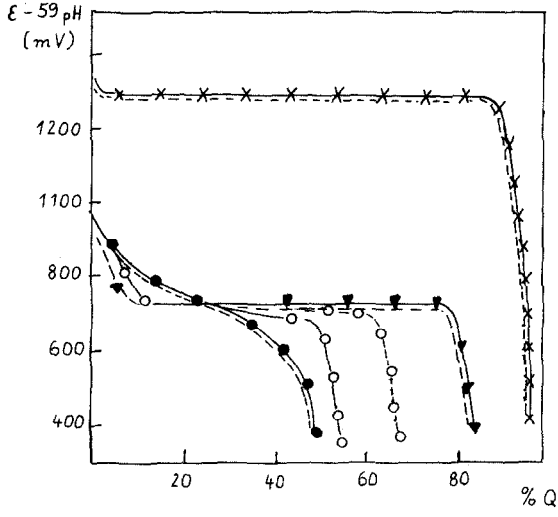

Fig. 2. Discharge curves with different electrolyte pH values in the range 0 - 15 as a function of the level of discharge, Q, (Mn(IV)/Mn(II)): j = 0.6 mA cm^{-2}. ——, ϵ-MnO_2; — — —, α-MnO_2; ●, pH 15; ○, pH 10; ▼, pH 4.5; ×, pH 0.

TABLE 2

Mn(II) formation

Structure	pH	Mn(II) (mole/mole MnO_2)
α, ϵ	0	1.0
α, ϵ	4 - 8	0.75
α	10	0.6
ϵ	10	0.2
α, ϵ	12 - 15	0

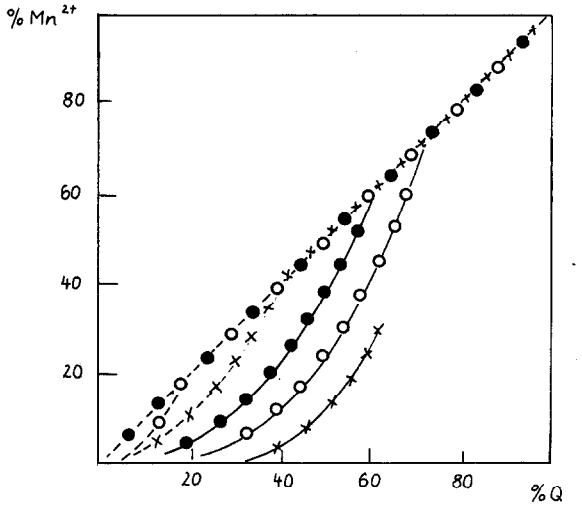

Fig. 3. Mn(II) formation *vs.* level of discharge, Q. ——, ϵ-MnO_2; — — —, α-MnO_2; ●, pH 4.5; ○, pH 8; ×, pH 10.

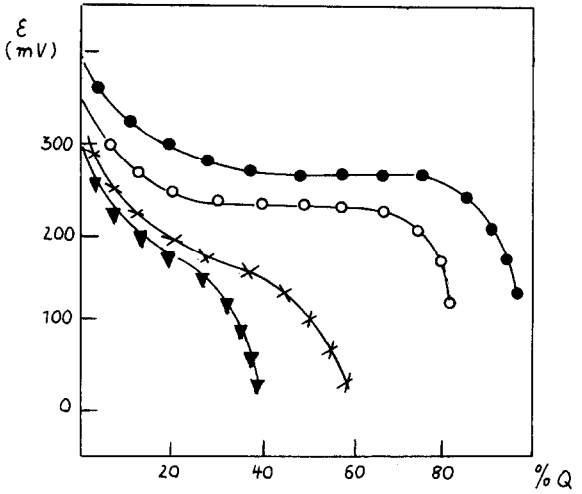

Fig. 4. Dependence of the discharge characteristic on the current density for α-MnO_2, pH 8. ●, 0.005 mA cm^{-2}; ○, 0.7 mA cm^{-2}; ×, 3 mA cm^{-2}; ▼, 3.5 mA cm^{-2}.

Fig. 5 we found agreement between the potential values at the start of the second section, whereas the degree of reduction at this point depends on the pH value. We conclude, therefore, that Mn(II) formation begins when the surface reaches a certain state of oxidation. If we compare the curves of Fig. 5. with the characteristics in a strong alkaline electrolyte, with only solid state reduction, we find the value $n = 1.75$ at the beginning of the second section. This value also can be derived from the voltage characteristic when the current densities, j, tend to zero as seen in Fig. 4.

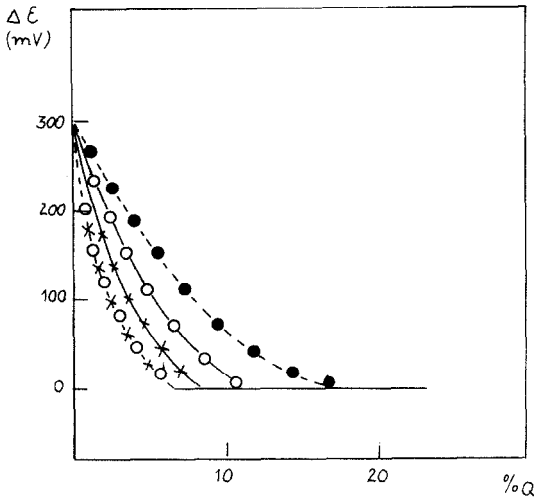

Fig. 5. Discharge characteristic over the initial stages of discharge. ——, ϵ-MnO_2; - - - -, α-MnO_2; ×, pH 4.5; ○, pH 8; ●, pH 10.

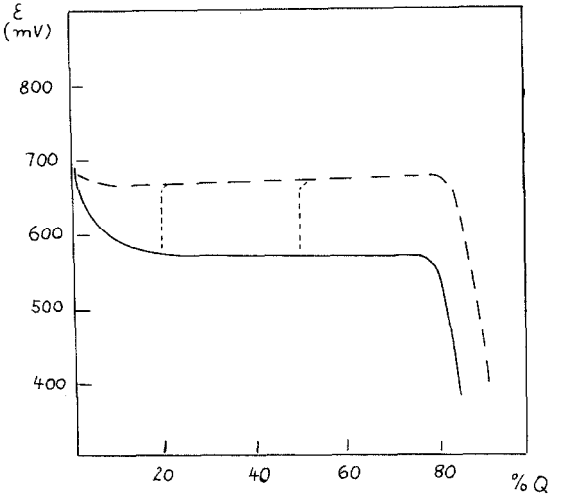

Fig. 6. Influence of zinc ions on the discharge characteristic of α-MnO_2; ——, 20% NH_4Cl; — — —, 20% NH_4Cl + 10% $ZnCl_2$; - - - -, NH_4Cl with added $ZnCl_2$.

In the presence of zinc ions the second section of the discharge curves of α-MnO_2 begins after a very short initial section, as shown in Fig. 6. Adding zinc ions during the discharge causes the potential to suddenly rise, indicating the formation of a new phase, which must be intermediate, since Mn(II) solution proceeds continuously.

In the pH range 4.5 - 12 the treatment of MnO_2 with 1 M Mn(II) solution leads to the product $MnOOH_{0.5}$. The reduced product remains

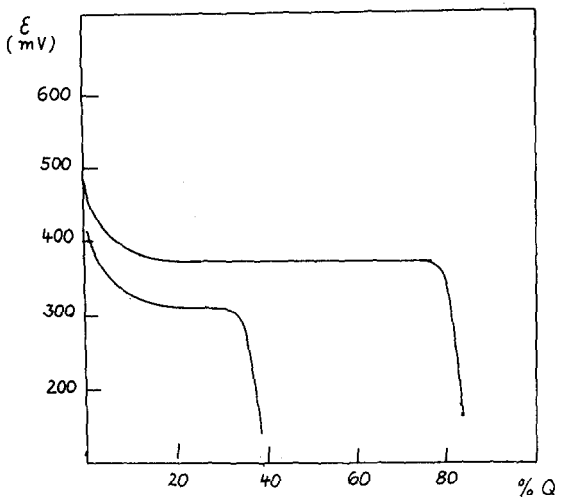

Fig. 7. Influence of Mn(II) treatment on the discharge characteristic of α-MnO_2 in pH 8. Right, untreated; left, after 60 h in 1 M Mn(II) solution at pH 12.

electrochemically active and has an initial section with a reducing voltage, indicating an homogeneous phase, see Fig. 7.

Discussion

From the experimental results we must consider four states with different voltage discharge characteristics:

(a) $pH < 4$

(b) $pH > 4$; $n \geqslant 1.75$

(c) $4 \leqslant pH \leqslant 12$; $1.75 \geqslant n \geqslant 1.5$

(d) $pH \geqslant 12$

From the results of Tari and Hirai [4], state (a) is represented by eqn. (5c) with the potential function:

$$\epsilon = \epsilon^0 + \frac{RT}{2F} \ln a(Mn^{2+}) - 0.118\ pH \tag{9}$$

As β-MnO_2, with 1×1 canals*, only reacts according to eqn. (5c), we assume that the disproportionation of MnOOH produces surface structures corresponding to β-MnO_2. From the cross reaction, (5c), the mechanism can be assigned to the electrolyte phase type.

In the range $pH \geqslant 4$ only a solid state mechanism proceeds up to $n = 1.75$ (state b). The voltage characteristic in this range is defined by eqn. (8), which is derived from statistical thermodynamics, assuming that changes in chemical energy do not occur. In reality, however, combined

*Corresponding to the definition given by Burns [2].

water influences crystal energy and the potential of MnO_2 according to eqn. (10), as reported by Preissler [14, 15]

$$\frac{dE}{dm} = -\frac{1}{F}\left(\frac{d\Delta G(m)}{dm}\right) \tag{10}$$

for an oxide $MnO_n \cdot mH_2O$ with the values $n = 1.96$ and $m = 0.23$ for EMD. For $m = 1$ and $m = 0.5$ ($MnO_n \cdot H_2O$ and $(MnO_n)_2 \cdot H_2O$), respectively) and adding the potential values of hydration from Preissler [14, 15] to eqn. (6), we get the characteristics presented in Fig. 8. In the second case we get good agreement with eqn. (8).

For the crystal structure of EMD with double chains which contain the combined water, we assume the following mechanism for the hydrated MnO_2:

$$MnO_2 \cdot MnO_2 \ldots H_2O \ldots MnO_2 \cdot MnO_2 \longrightarrow$$

$$MnO_2 \cdot MnOOH \ldots H_2O \ldots MnOOH \cdot MnO_2 \tag{11}$$

respectively:

$$MnOOH_r \cdot mH_2O + 2mH^+ + 2me \longrightarrow MnOOH_{r+2m} \cdot mH_2O \tag{12}$$

With $r = 0$ and $m = 0.25$, it follows from eqn. (12)

$$MnO_2 \cdot 0.25H_2O + 0.5H^+ + 0.5e \longrightarrow MnOOH_{0.5} + 0.25H_2O \tag{13}$$

and we get the potential function:

$$\epsilon = \epsilon^0 + \frac{RT}{1/2F} \ln \frac{1-x}{x} + \frac{RT}{1/2F} \ln a(H^+)^{1/2} \tag{14}$$

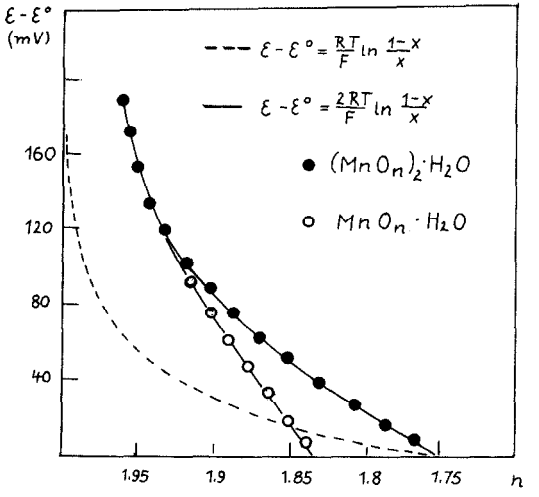

Fig. 8. Discharge characteristics of $MnO_n \cdot H_2O$ and $(MnO_n)_2 \cdot H_2O$ with the hydration potential added.

Equation (14) is identical with eqn. (8) but, since eqn. (14) was deduced from a consideration of the hydration energy, the voltage characteristic cannot be interpreted by eqn. (7) using a change in configuration entropy.

In the pH-range 5 - 10 (state c) Mn(II) formation cannot arise from disproportionation, since equilibrium (5b) lies on the left-hand side. Mn(II) therefore must be produced electrochemically. Assuming the formation of $Mn(OH)_2$ to be a second phase on the surface at the point $n = 1.75$, we get the following equations:

$$MnO_2 + H^+ + e \longrightarrow MnOOH \tag{15}$$

$$\epsilon^0\text{hom.} = \frac{1}{F}\left(G^0(MnO_2) - G^0(MnOOH)\right) + \frac{RT}{1/2F} \ln a(H^+)^{1/2} \tag{16}$$

$$MnOOH_{0.5} + 1.5H^+ + 1.5e \longrightarrow Mn(OH)_2 \tag{17}$$

$$\epsilon^0\text{het.} = \frac{1}{1.5F}\left(G^0(MnOOH_{0.5}) - G^0(MnOH)_2\right) + \frac{RT}{1.5F} \ln a(H^+)^{1/2} \tag{18}$$

With $G^0(MnOOH_{0.5}) = 377.6$ kJ and $G^0(MnOH)_2) = 504.9$ kJ it follows that for $n = 1.75$:

$$\epsilon^0\text{hom.} = \epsilon^0\text{het.} = 0.86 \text{ V} \tag{19}$$

At the point $n = 1.75$, $Mn(OH)_2$ formation is thermodynamically favored. The nearly constant potential indicates a reduction in the heterogeneous phase. During discharge this phase must have an intermediate state, since Mn(II) formation is continuous. A similar intermediate surface phase was indicated by Fig. 6 for α-MnO_2 in the presence of zinc ions. The formation of the $Mn(OH)_2$ phase under the conditions of state (c) depends on the equilibrium:

$$MnOOH_r(\text{latt.}) \rightleftharpoons Mn(OH)_2(\text{surf.}) \overset{NH_4^+}{\rightleftharpoons} Mn(NH_3)_2^{2+}(\text{sol.}) \tag{20}$$

In electrolytes with pH $\geqslant$ 12 no Mn(II) dissolution occurs. The voltage characteristic does not agree with eqn. (6), corresponding to MnOOH formation according to eqn. (4), as shown in Fig. 9. From eqn. (19) $Mn(OH)_2$ formation is also to be expected under the conditions of state (d), but it must be followed under these conditions by dismutation:

$$MnOOH_{0.5} + \Delta H^+ + \Delta e \longrightarrow (1 - \Delta)MnOOH_{0.5} + \Delta Mn(OH)_2 \tag{21}$$

$$MnOOH_{0.5} + \Delta Mn(OH)_2 \longrightarrow MnOOH_{0.5+2\Delta} \tag{22}$$

If the $Mn(OH)_2$ formation proceeds on the surface of the homogeneous phase, we have to consider the following equilibrium

$$\begin{array}{|c|c|} \hline MnO_2 \cdot MnOOH & \rightleftharpoons\!\!\!\!\rightleftharpoons\; MnO_2 \cdot Mn(OH)_2 \\ & \Downarrow \\ & MnOOH \cdot MnOOH \\ \hline \end{array} \tag{23}$$

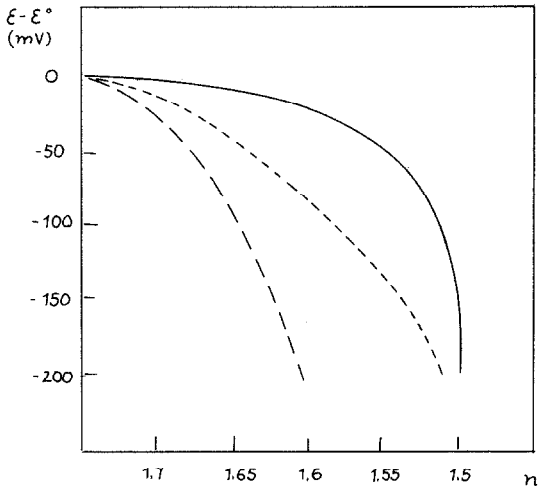

Fig. 9. Discharge characteristics over the latter stages of discharge. ——, $\epsilon - \epsilon^0 = 0.059 \ln 1 - x/x$; — — —, discharge characteristic from Atlung [3]; - - - -, discharge characteristic from Tye [8].

Thus, the degree of oxidation differs between lattice and surface and affects the voltage characteristic in the range $n < 1.75$. The experimental voltage characteristics used by Atlung [3] and Tye [8] do not agree, as seen in Fig. 9. This may be more due to the influence of the experimental conditions on equilibrium (23), than to changes in the configuration entropy.

MnOOH diffusion proceeds by the diffusion of protons and electrons. From the studies of β-MnO_2, with 1×1 channels and reacting by the electrolyte phase mechanism, we know that proton diffusion into the lattice is only possible if there are channels greater than 1×1. ϵ-MnO_2, therefore, being a mixed structure of pyrolusite (1×1 channels) and ramsdellite (1×2 channels) [2], does not have the necessary numbers of channels for proton diffusion. With regard to eqn. (11) we assume a proton transfer *versus* MnOOH for the second section according to:

$$H^{\cdot} \longrightarrow H_2O \overset{\frown}{\ldots} MnOOH \cdot MnO_2 \overset{\frown}{} \qquad (24)$$

For the electrode reaction of the $NiOOH/Ni(OH)_2$ system where:

$$NiOOH + H^{\cdot} + e \longrightarrow Ni(OH)_2 \qquad (25)$$

a proton diffusion mechanism is generally assumed. NiOOH has a lattice structure with combined water. Figure 10 compares voltage discharge characteristics of ϵ-MnO_2 and of NiOOH from Jones [16]. Whereas the curves generally follow each other during their initial discharge they then diverge. From the X-ray investigations of Briggs [17] it is known that the first half of the discharge proceeds in an homogeneous phase, whereas, in the second half, $Ni(OH)_2$ arises as an heterogeneous phase. Thus NiOOH is

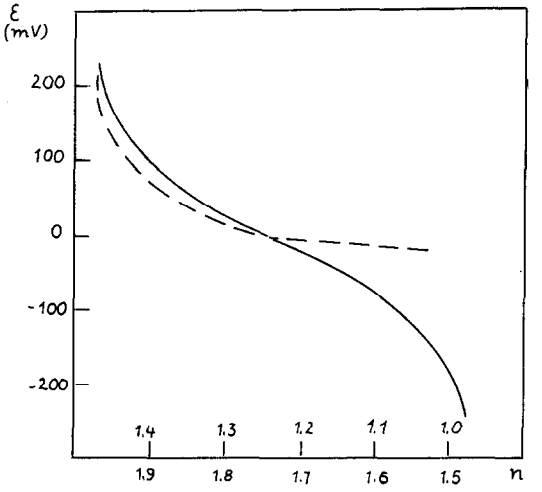

Fig. 10. Comparison of the discharge characteristics of MnO_2 and NiOOH. ——, MnO_2; — — —, NiOOH.

the same as MnO_2 in that the homogeneous phase only covers the range of $0.5F$ according to the equation:

$$NiOOH + 0.5H^+ + 0.5e \longrightarrow NiOOH_{1.5} \tag{26}$$

The differential behavior in the second part of the discharge may result from the fact that a reaction with the homogeneous phase by dismutation similar to $MnO_2/Mn(OH)_2$ is not possible for NiOOH.

The voltage characteristic of MnO_2 in aprotic Li^+ electrolytes principally differs from that in aqueous electrolytes, as shown in Fig. 11 based on the results of Nardi [18]. According to the reaction:

$$MnO_2 + xLi^+ + xe \longrightarrow Li_xMnO_2 \tag{27}$$

the potential is constant in the range $0.1 < x \leqslant 0.4$. This is interpreted as reduction in the heterogeneous phase. The voltage characteristic also changes with recovery time: the length of the voltage plateau is reduced as the recovery time is limited. As the recovery time during the first half of the discharge is much greater than during the second half, Nardi assumes a more rapid movement of lithium ions in the latter stage. This conclusion agrees with the discussed difference in proton transfer during the second stage of discharge in aqueous solution. Hydration of MnO_2 influences the voltage discharge characteristic in an aprotic electrolyte in the same way as in an aqueous solution [18].

Figure 11 additionally shows the voltage characteristics of Na_xWO_3 and Li_xMoO_3 from Wittingham [19]. That of WO_3 corresponds to the one of MnO_2, whereas the potential of MoO_3 (and also V_2O_5) diminishes linearly with the degree of reduction. The different types of voltage characteristic correspond to different types of structure. WO_3 consists of MO_6 chains

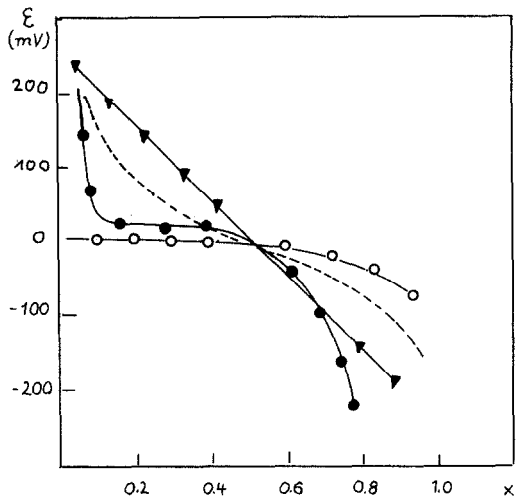

Fig. 11. Discharge characteristics of oxide electrodes in aprotic electrolytes. ●, MnO_2/Li^+; ○, WO_3/Na^+; ▼, MoO_3/Li^+; - - - -, MnO_2 in aqueous electrolyte.

forming channels corresponding to MnO_2 whereas MoO_3 and V_2O_5 have sandwich layers with van der Waals bonding like dichalcogenides [20]. The movement of lithium ions is more rapid in structures with sandwich layers [20].

From the discussed results we conclude that the discharge characteristic of insertion electrodes is determined by the structural properties and by the type of bonding of the inserted cation. Three states can be distinguished:

— hydrated oxides with channels, forming MO_6 chains, or a layer structure with hydrogen bridge bonding of the inserted cation and with movement by the Grotthus mechanism;

— oxides with OMO sandwich layers and weakly bonded inserted cations in the gaps between the layers;

— MO_6 chains with channels containing the inserted cations, characterized by slow movement.

The homogeneous phase of MnO_2 is usually deduced on the basis of an homogeneous mixture of MnO_2 and MnOOH. It seems that this presumption in the third type, with slow movement of the inserted cation, is not justified.

Conclusion

Insertion electrodes cannot be described by a general expression based only on distribution entropy. It seems possible, however, to assume three types of oxide, each with a typical voltage discharge characteristic, differing in the type of bonding of the inserted cation in the lattice.

List of symbols

φ	Charge density
c_S	Specific capacity
ρ_K	Crystallographic density
G	Gibbs energy
ϵ	Electrode voltage
H	Enthalpy
S	Entropy
W	Probability
R	Gas constant
x	Mole fraction
n	Degree of reduction
$q(Q)$	State of discharge
q_i	Factor reducing the charge density
q_e	Factor reducing charge density by voltage discharge characteristic
U	Cell voltage
zF	Faraday efficiency for an electrode reaction with z electrons.
j	Discharge current.

References

1 H. W. Uhlig, *Z. Phys. Chem., Leipzig*, in press.
2 R. G. Burns and V. M. Burns, *Proc. Manganese Dioxide Symposium, Tokyo, 1980*, Vol. 2, J. C. Sample Office, Cleveland, OH, p. 97.
3 S. Atlung and T. Jacobsen, *Electrochim. Acta, 26* (1981) 1447.
4 I. Tari and T. Hirai, *Electrochim. Acta, 27* (1982) 235.
5 P. Ruetschi, *J. Electrochem. Soc., 131* (1984) 2737.
6 R. S. Johnson and W. C. Vosburgh, *J. Electrochem. Soc., 99* (1952) 317.
7 W. C. Maskell, J. E. Shaw and F. L. Tye, *Electrochim. Acta, 28* (1983) 225.
8 F. L. Tye, *Electrochim. Acta, 30* (1985) 17.
9 J. P. Gabano, B. Morignat and J. F. Laurent, in D. H. Collins (ed.), *Power Sources 1966*, Pergamon Press, Oxford, 1967, p. 49.
10 N. C. Cahoon and M. Korver, *J. Electrochem. Soc., 106* (1959) 745.
11 W. C. Maskell, J. E. Shaw and F. L. Tye, *Electrochim. Acta, 28* (1983) 231.
12 H. W. Uhlig, *Z. Phys. Chem., Leipzig, 265* (1984) 497.
13 G. Kanoh and M. Takaoka, *Proc. Manganese Dioxide Symp., Tokyo, 1980*, Vol. 2, J. C. Sample Office, Cleveland, OH, p. 134.
14 E. Preissler, *Proc. Manganese Dioxide Symp., Tokyo, 1980*, Vol. 2, J. C. Sample Office, Cleveland, OH, p. 184.
15 E. Preissler, *J. Appl. Electrochem., 66* (1976) 311.
16 E. Jones and W. F. K. Wynne-Jones, *Trans. Faraday Soc., 52* (1956) 1260.
17 G. W. D. Briggs and W. F. K. Wynne-Jones, *Trans. Faraday Soc., 52* (1956) 1272.
18 J. C. Nardi, *J. Electrochem. Soc., 132* (1985) 1787.
19 M. S. Wittingham, *J. Electrochem. Soc., 122* (1975) 713.
20 P. C. Dickens and G. J. Reynolds, *Solid State Ionics, 5* (1981) 331.